JOURNAL OF GEOPHYSICAL RESEARCH, VOL. 112, C10010, doi:10.1029/2006JC003954, 2007

Control of salinity on the mixed layer depth in the world ocean: 2. Tropical areas

Juliette Mignot,[1] Clement de Boyer Montégut,[2] Alban Lazar,[1] and Sophie Cravatte[3]

Received 6 October 2006; revised 22 February 2007; accepted 22 March 2007; published 10 October 2007.

[1] A new global climatology of the barrier layer (BL) thickness based on the analysis of instantaneous temperature and salinity profiles was presented in the first part of this paper. It is used here to revisit the mean properties of the phenomenon in the tropics. Consistent with previous studies, thick and persistent BLs are detected in the deep tropics of each ocean. Their formation involves various mechanisms such as intense precipitations, oceanic circulation, wind seasonality, and river runoff, in relation with the specific geography and climatology of each basin. The weak seasonal cycle of the BL in the equatorial Pacific is analyzed in particular. Thick BLs are also detected in winter on the equatorial flank of each of the subtropical salinity maxima. They are due to the specific salinity stratification in this area and to the seasonal homogenization of temperature over the vertical under the action of atmospheric heat fluxes. Thick BLs in the western tropical Atlantic that are partly associated with important vertical temperature inversions are furthermore identified and described. More generally, agreement of the BLs mean properties in these areas with previous literature confirms the robustness of the features and validates this new product that uses most available data including the most recent ones issued from the ARGO floats.

Citation: Mignot, J., C. de Boyer Montégut, A. Lazar, and S. Cravatte (2007), Control of salinity on the mixed layer depth in the world ocean: 2. Tropical areas, *J. Geophys. Res.*, *112*, C10010, doi:10.1029/2006JC003954.

1. Introduction

[2] In a companion paper, *de Boyer Montégut et al.* [2007a] present a new global climatology of the Barrier Layer (BL) features and associated vertical temperature inversions phenomenon. This global presentation allowed us to distinguish three types of BL regions. They are quasipermanent in most of the equatorial and deep tropical (i.e., equatorward of roughly 10°) basins but also the Labrador Sea and parts of the Arctic and Southern Ocean. They appear rather seasonally in the northern subpolar basins, the tropical-subtropical basins and the Arabian Sea. Finally in the regions between 25° and 45° latitude, BLs are detected only very locally.

[3] Former studies of the BL have mainly focused on the tropical oceans where its potential climatic impact is particularly strong. At low latitudes indeed, the mixed layer is relatively shallow and thus can be easily eroded. In the presence of a BL in subsurface, this can induce a positive sea surface temperature anomaly that was suggested to influence significantly the local air-sea interactions [e.g., *Vialard and Delecluse*, 1998a]. Ocean-atmosphere coupling is indeed known to be strongest at low latitudes, so that extraordinary conditions in the upper oceanic layer are likely to have a significant influence on the atmosphere above. In particular, BLs may contribute to maintain the heat buildup necessary for El Niño development [*Wyrtki*, 1975; *Meinen and McPhaden*, 2000; *Maes et al.*, 2005] and thus play an important role on the onset of El Niño–Southern Oscillation (ENSO) events [e.g., *Maes et al.*, 2002, 2004]. Recent studies also highlighted the link between oceanic BLs and the development of the Indian monsoon [*Masson et al.*, 2005].

[4] In an early study, *Sprintall and Tomczak* [1992] greatly contributed to the knowledge and understanding of tropical BL climatology. Yet, essentially because of the lack of data, their work was based on already averaged and interpolated data sets, which result in smoothed vertical profiles and can thus create artificial mixing of water masses. It can also introduce biases in estimating subsurface quantities linked to stratification as shown by *de Boyer Montégut et al.* [2004]. Since then, various authors have used individual profiles, thereby retaining more detailed structures, but their studies only concerned limited areas [e.g., *Ando and McPhaden*, 1997; *Sato et al.*, 2004, *Qu and Meyers*, 2005]. Recently, *Sato et al.* [2006] used the Argo floats profiles collected from January 2000 to June 2005 to investigate the BLs in the subtropical gyres of the world's oceans. Their study shed light on patchy and thicker structures than the ones revealed by gridded climatologies. Here we use a large data set based on most temperature and

[1] Laboratoire d'Océanographie et de Climatologie: Éxperimentation et Approches Numérique (CNRS/IRD/UPMC/MNHN), Institut Pierre Simon Laplace, Paris, France.
[2] Frontier Research Center for Global Change (JAMSTEC), Yokohama, Japan.
[3] Laboratoire d'Études en Géophysique et Océanographie Spatiales (CNRS/IRD/UPS/CNES), Toulouse, France.

0148-0227/07/2006JC003954$09.00

salinity profiles available since 1967, including in particular the ones used by *Sato et al.* [2006]. The point is to use a data set as accurate as possible to test the robustness of the features detected in previous studies, to investigate the possible presence of new, unknown BLs and to gain understanding on the seasonality of BL thickness and frequency in the tropics (equatorward of roughly 25° latitude).

[5] The data set is briefly presented in the following section. A full description is given by *de Boyer Montégut et al.* [2007a]. We then describe and analyze the BL climatology in the Pacific and the Atlantic deep tropics (sections 3 and 4, respectively). Section 5 is dedicated to BLs of the northern tropical Indian Ocean (north of 10°S). BLs appearing farther poleward, between 10 and 20° latitude are analyzed in sections 6 and 7. The analysis by *de Boyer Montégut et al.* [2007a] shed light on strong similarities regarding seasonality and formation mechanisms of some BL areas. We will show (section 6) that this is particularly true for this latitude band (except for the northern Indian ocean due to its specific geometry). A specific and strong BL of the Atlantic warm pool is analyzed separately (section 7). Conclusions are given in section 8.

2. Data Set

[6] This study is based on the collection of more than 500,000 instantaneous temperature and salinity profiles collected between 1967 and 2006. They were obtained from the National Oceanographic Data Center (NODC), from the World Ocean Circulation Experiment (WOCE) database, and complemented by those available between 1996 and 2006 from the ARGO database. The first two databases were used by *de Boyer Montégut et al.* [2004] to construct a new global temperature-based mixed layer depth climatology. The latter leads to an increase of 30% of the database. The reader is referred to *de Boyer Montégut et al.* [2004, 2007a] for a detailed description of the data processing. We recall that the BL thickness is defined as the difference $D_{T-02} - D_{\sigma}$. D_{T-02} is the depth where the temperature has decreased by 0.2°C as compared to the temperature at the reference depth of 10 m, D_{σ} is the depth where the potential density has increased from the reference depth by a density threshold equivalent to the same temperature change 0.2°C at constant salinity (equation (1) of *de Boyer Montégut et al.* [2007a]).

3. Deep Tropical Pacific

[7] A barrier layer is present all year long in the Warm Pool, also defined as the Fresh Pool [*Hénin et al.*, 1998], of the western equatorial Pacific, and under the South Pacific Convergence Zone (SPCZ) (Figure 1). It is also present seasonally across the whole basin under the Inter-Tropical Convergence Zone (ITCZ). The formation mechanisms of the tropical Pacific BLs are complex and result from interactions between atmospheric forcing, small and large-scale oceanic processes [*Cronin and McPhaden*, 2002]. In spite of the numerous studies dedicated to this area, the seasonal cycle of the BL in the tropical Pacific is poorly documented. We analyze it below before focusing on the equatorial region. As mentioned above, BLs in the latter are indeed particularly important for local air-sea processes and large-scale phenomena such as ENSO [e.g., *Maes et al.*, 2002].

3.1. Seasonal Cycle of the Tropical Pacific BLs

[8] To our knowledge, the seasonal cycle of the BL in the tropical Pacific has only been described by *Sprintall and Tomczak* [1992]. The reason might be that at the Equator, the BL thickness is in fact rather modulated at intraseasonal (Madden Julian Oscillations or Westerly Wind Events) or interannual (ENSO events) than at seasonal timescales. For comparison with the work of *Sprintall and Tomczak* [1992], we plotted in Figure 2 the barrier layer thickness for the same seasons and region as in *Sprintall and Tomczak*'s [1992] Figure 2. Note that a perfect match between the two data sets is not to be expected because of their use of a different stratification criterion (0.5°C) and of already interpolated profiles. Our product generally yields thinner BLs but their location is nevertheless in good general agreement. Figure 2 also illustrates that BLs in the tropical Pacific exhibit a clear seasonal cycle.

[9] In late boreal winter (February to April), BLs are primarily concentrated in the western equatorial basin, between 10°S and 10°N, and under the SPCZ. During the following six months, the BL thickness in the western Southern Hemisphere decreases while that in the Northern Hemisphere, along 5°N, persists and extends almost across the whole basin. This seasonal evolution closely follows that of the low sea surface salinity (SSS) patterns [*Delcroix et al.*, 1998] as well as the seasonal displacement and reinforcement of the intense precipitations (black contours in Figure 2) associated to the ITCZ in the northern equatorial basin and to the SPCZ in the southern tropics. This is the primary formation mechanism in this region, as described by *You* [1995]. *Durand et al.* [2002] showed that weaker winds associated with these enhanced precipitations lead to a stronger shoaling of the mixed layer than the isothermal layer thus enhancing the BL thickness. Furthermore, the penetration of the radiative heat flux through the thin mixed layer also probably contributes to maintain the temperature of the subsurface layer [*Woods et al.*, 1984; *Lewis et al.*, 1990; *Vialard and Delecluse*, 1998b].

[10] In late boreal winter (February to April), an important BL is also observed farther north (15°N–20°N) in the central Pacific. *Sprintall and Tomczak* [1992] also detected this BL, and argued that it is related to the movement of the ITCZ. Yet, it is not located under the ITCZ-induced precipitation region at this time period (Figure 2). Symmetrically, BLs are detected near 15°S between May and October east of 150°W, far away from the precipitations associated to the SPCZ. These phenomena are further investigated in section 6.

3.2. Equatorial Pacific BLs

[11] Figure 3 (left) shows that along the equator, barrier layers deeper than 15 m are mostly confined to the Warm Pool region, where SSTs and precipitations are maximum and SSSs are minimum. Two seasonal features are particularly evident in Figure 3 and are discussed below successively: BLs located at the eastern edge of the Warm Pool (section 3.2.1) and BLs located in the far western equatorial Pacific (130°E–150°E) in boreal summer (section 3.2.2).

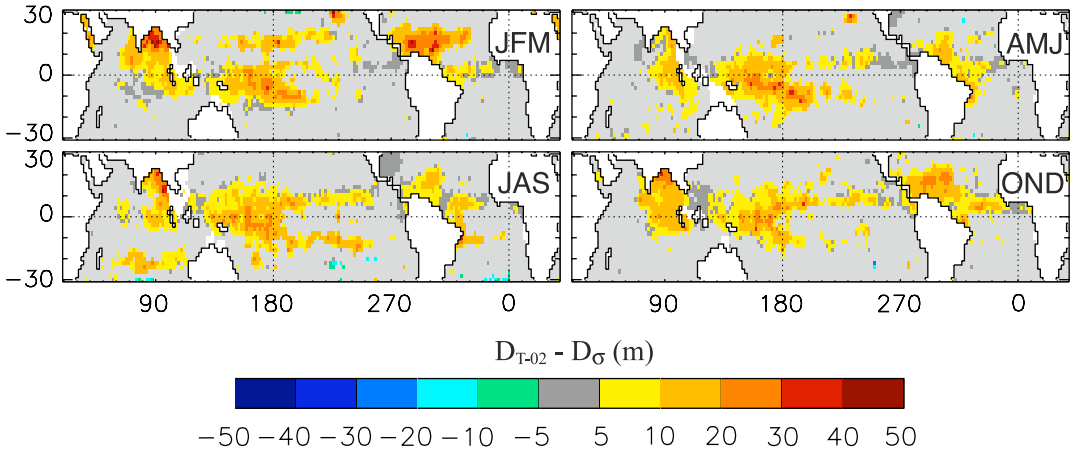

Figure 1. Seasonal maps of the difference between $D_{T\text{-}02}$ and D_σ for the tropical band. Positive values correspond to Barrier Layer thickness, negative values correspond to compensated layer thickness (see Part 1 [*de Boyer Montégut et al.*, 2007a] for discussion about the latter). Data have been kriged every month following *de Boyer Montégut et al.* [2004]. Grid points where the layer thickness is less than 10% than the maximal depth ($D_{T\text{-}02}$ or D_σ) are shown in light grey. White areas (except the continents) represent grid points with no data or only 1 month of data during the season. Seasonal averages are given for (top left) January to March (JFM), (top right) April to June (AMJ), (bottom left) July to September (JAS), and (bottom right) October to December (OND).

The isolated occurrence of thick BLs in the eastern Pacific ([130°W–140°W]) in September to November corresponds to measurements taken during strong El Niño events. This demonstrates the impact of ENSO events on the upper vertical stratification in the equatorial Pacific. When the BL climatology is recomputed excluding El Niño years, these BLs in the eastern Pacific are not present anymore (not shown).

3.2.1. Warm Pool BLs

[12] The Warm Pool BLs are relatively sharply cut off to the west, along a seasonally varying line around 170°E–180°E. This line seems to be defined well by the seasonal variations of the 35 psu and 29°C isolines (Figure 3, left, solid and dotted lines, respectively), taken as proxies for the eastern edge of the Warm-Fresh Pool. Such a link has already been observed at interannual timescales [*Ando and McPhaden*, 1997; *Cronin and McPhaden*, 2002] and noticed at seasonal timescales in a forced [*Durand et al.*, 2002] and a coupled model [*Maes et al.*, 2005], though with a different timing. It cannot be explained by seasonal variations of precipitations which are small in this region [*Delcroix et al.*, 1998] and not in phase with the seasonal displacement of the

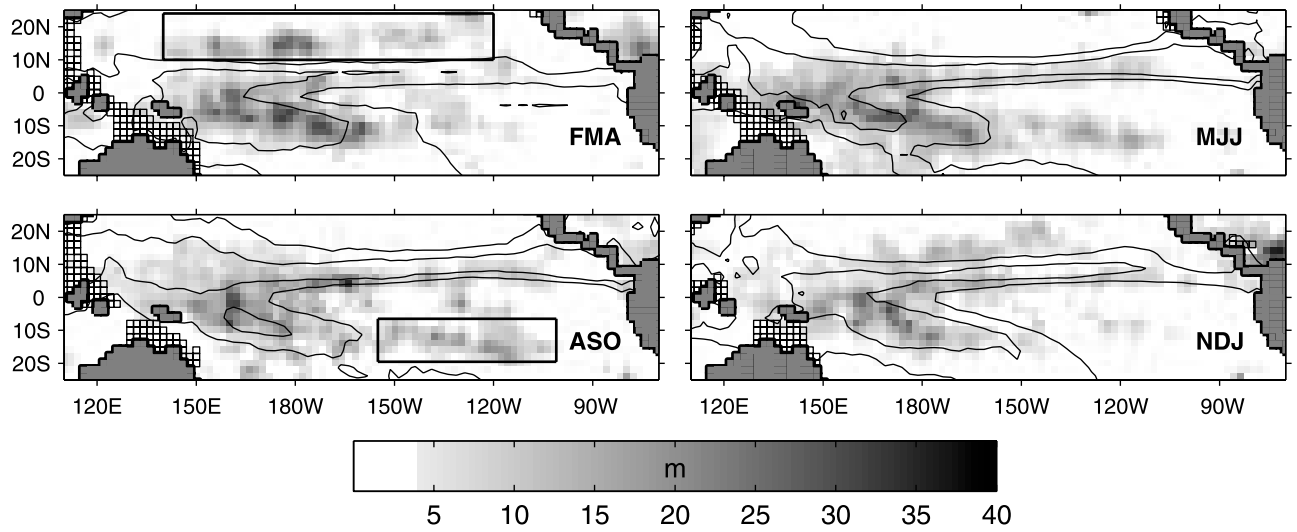

Figure 2. Grey scale gives BL thickness during the same seasons as used by *Sprintall and Tomczak* [1992]. Grid points with no data during at least 1 month of the season are shown contoured in black. Contours are 4 mm/d and 8 mm/d precipitation contours from the *Xie and Arkin* [1997] data set. The boxes highlight BL areas studied in section 6 and also shown in Figure 6.

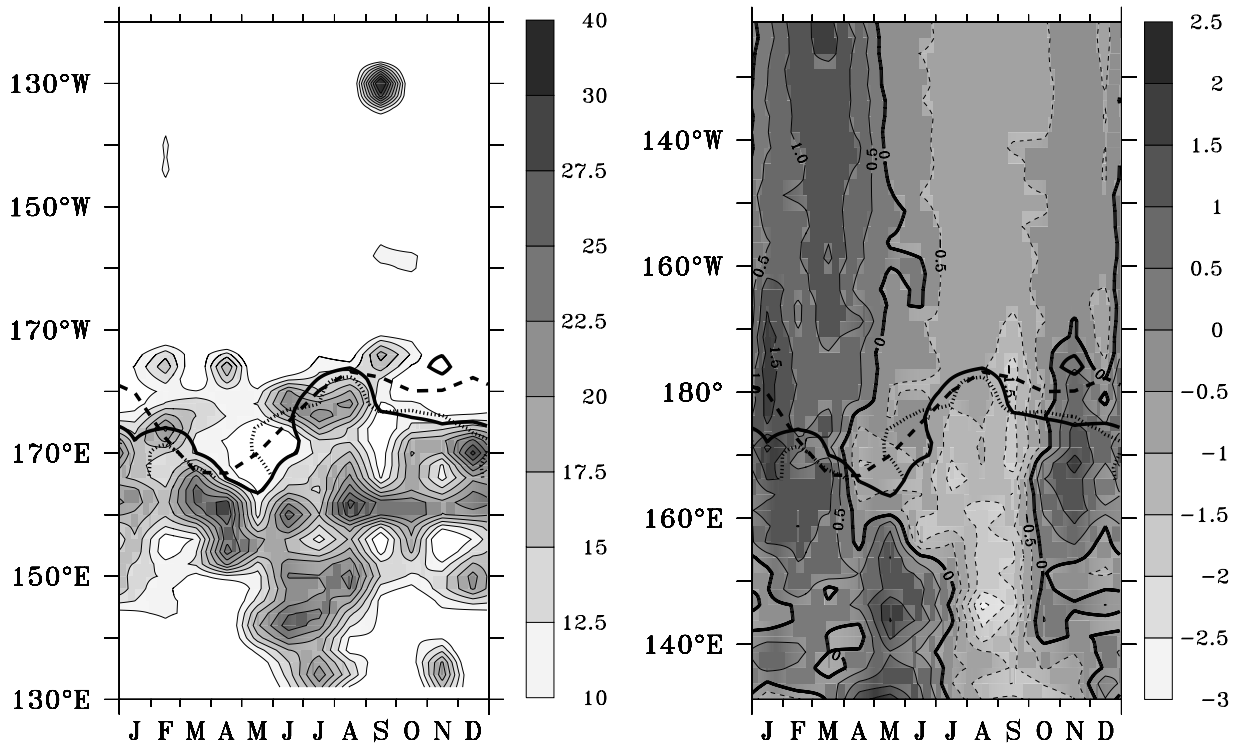

Figure 3. (left) Barrier layer thickness averaged between 2°S–2°N as a function of longitude and climatological months in the Pacific. (right) Same for the CMAP precipitations (mm/d) after substraction of the annual mean. For clarity, the fields have been smoothed using a three-point hanning window before computing the latitudinal average. On both plots the solid line shows the climatological 35 psu isohaline and the dotted line shows the 29°C isotherm averaged between 2°S and 2°N and computed with the same data sets as the BL. The dashed line shows the zero line of zonal currents seasonal anomalies (OSCAR product [*Bonjean and Lagerloef*, 2002]; annual mean has been removed) near the eastern edge of the warm pool integrated in time. Thus it indicates the zonal displacement of the eastern edge of the warm pool due to zonal advection only.

Warm-Fresh Pool (Figure 3, right). It is more probably related to that of the currents as shown by the time integral of the seasonal anomalies of the zonal velocity near the eastern edge of the Warm Pool plotted in Figure 3 (dashed line). From February to April, mean currents are westward in the western Equatorial Pacific [*Reverdin et al.*, 1994]. The eastern edge of the Warm Pool retreats to the west, as well as the BL area. From April to July, trade winds relax and the situation is reversed.

[13] The predominance of zonal advection as mechanism for the displacements of the eastern edge of the Warm-Fresh Pool was shown by *Picaut et al.* [2001] at interannual timescales. Understanding whether this seasonality is the signature of a phase locking of interannual variability to the seasonal cycle or is related to an intrinsic seasonality of the equatorial Pacific requires further study. However, analysis of BL climatologies excluding successively El Niño years, La Niña years and both argue for a predominant intrinsic variability. It is also worth noting that the BL thickness at the eastern edge of the warm pool is maximum in December, when equatorial westerly wind events are more frequent [*Harrison and Vecchi*, 1997] and create a mean eastward zonal current in the Warm Pool, whereas the westward flowing South Equatorial Current is strong [*Reverdin et al.*, 1994]. Our product is thus consistent with the hypothesis that BLs of the Warm Pool are mostly formed by the tilting/shearing mechanism or by subduction of salty water in the convergence zone [*Lukas and Lindstrom*, 1991; *Shinoda and Lukas*, 1995; *Vialard and Delecluse*, 1998a], and support the idea that maximum current convergence may create thicker BLs linked to intensified subduction. The collocation between warm SSTs, salinity front, and thick BLs observed in Figure 3 confirm that the BL may feed back on the ocean-atmosphere interactions and modify the SSTs, as suggested by previous studies [*Picaut et al.*, 2001; *Maes et al.*, 2006].

3.2.2. Far Western Equatorial BLs

[14] Thick BLs are also observed in the far western equatorial Pacific (west of 150°E) in June to August (Figure 3). They are also present in a climatology computed excluding La Niña years (not shown) so that their presence cannot be attributed to a bias due to these events. Its formation is rather consistent with the seasonal freshening linked to the increase of precipitations from March to June and its destruction with the decrease of precipitations in fall and the increase of wind-induced mixing (Figure 3). Note that *Delcroix and McPhaden* [2002] proposed an interesting formation mechanism at interannual timescales based on the possible role of downwelling Rossby waves that deepen the thermocline, and thus the isothermal layer, but not the mixed layer, since vertical velocities associated with Rossby waves are larger at

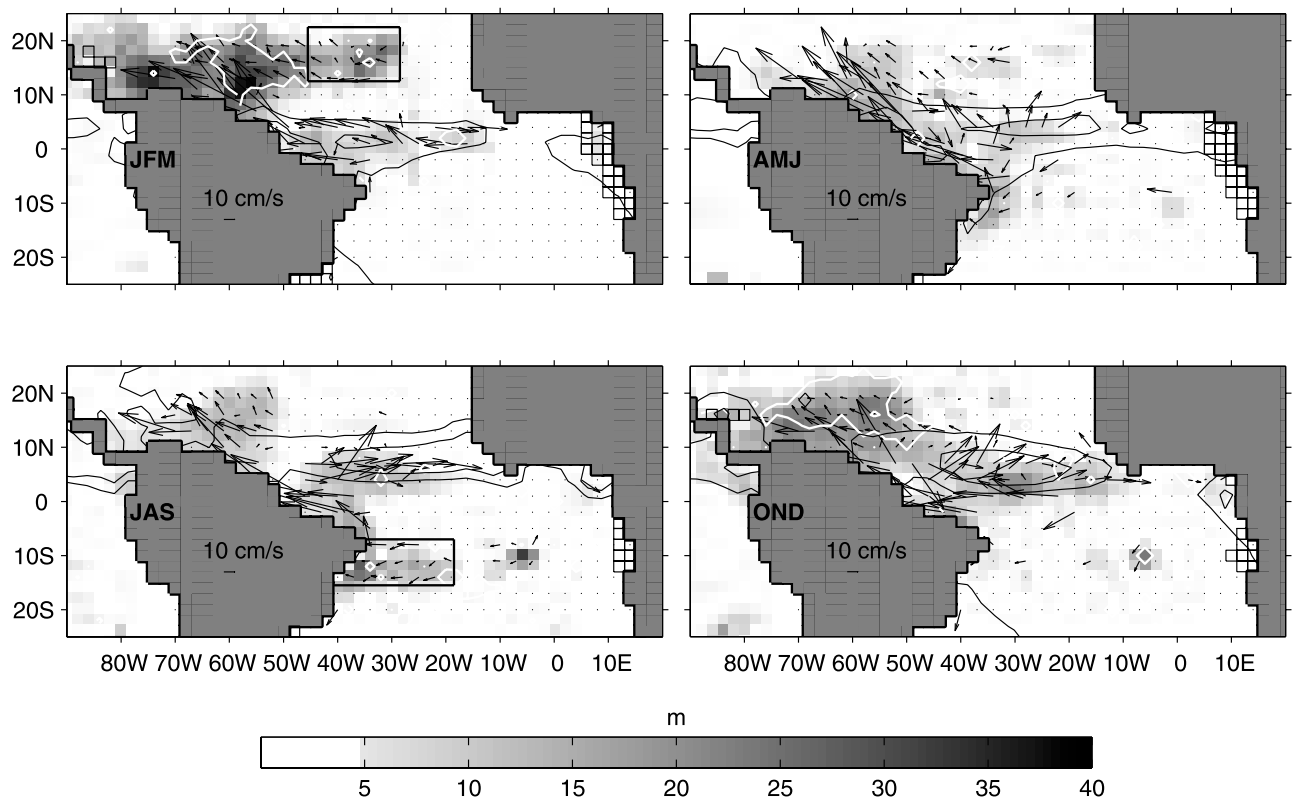

Figure 4. Grey scale gives easonal BL thickness in the tropical Atlantic basin. Grid points with no data during at least 1 month of the season are shown contoured in black. Arrows denote drifter-derived seasonal near-surface currents from *Lumpkin and Garraffo* [2005]. For clarity, the currents have been smoothed using a three-point hanning window over both dimensions, and only one vector out of three is shown, and only at areas where the BL is thicker than 5 m. Black contours are 4 mm/d and 8 mm/d precipitation contours from the *Xie and Arkin* [1997] data set. White contours are subsurface temperature maximum greater than 0.3°C over the season (see *de Boyer Montégut et al.* [2007a] for details). The four panels represent an average over the four seasons as in Figure 1. The boxes highlight BL areas studied in section 6 and also shown in Figure 6.

deeper depths. This would then induce a thickening of the BL by vertical stretching. However, in July–August, it is rather annual upwelling Rossby waves that reach the western Pacific [*Yu and McPhaden*, 1999]. Therefore our product confirms the existence of these thick BLs but do not support this formation hypothesis at seasonal timescales.

4. Deep Tropical Atlantic

[15] The salinity budget of the equatorial and tropical Atlantic is relatively complex [e.g., *Foltz et al.*, 2004; *Ferry and Reverdin*, 2004] and two major sources of freshwater have to be taken into account: high precipitations under the ITCZ, and the discharge of major rivers along the northern coast of South America, namely the Amazon (0°N–50°W) and, to a lesser extent, the Orinoco (9.25°N–61.5°W). Barrier layers of up to 20 m thickness are detected in the deep tropical Atlantic basin, equatorward of roughly 10° latitude (Figure 4). Two areas can be distinguished: the coastal zone from Guyana to Venezuela (roughly 200 to 300 km offshore) and the equatorial zone (5°S–10°N). They have already been analyzed using observations [*Pailler et al.*, 1999] and models [e.g., *Masson and Delecluse*, 2001; *Ferry and Reverdin*, 2004], and are further described below.

[16] In boreal winter and spring (Figure 4, top), the fresh Amazon waters are advected northwestward by the Guyana current [e.g., *Condie*, 1991], inducing a shallow halocline along the northern coast of South America. The latter is further strengthened by local precipitations, as indicated by the thick black line in Figure 4. Since the temperature is relatively constant along this path in the Atlantic warm pool, this results in the BL detected along the coast in October to March north of the Amazon mouth (located at 0° latitude). This mechanism has been described by *Pailler et al.* [1999] in particular, using high-resolution vertical profiles. The latter also suggested that in summer, the North Equatorial Current retroflection carries the Amazon waters across the basin at 6°N [e.g., *Lentz*, 1995; *Hu et al.*, 2004] here again practically along the isotherms (not shown). Our product supports this explanation at large scale. Figure 4 shows indeed thick BLs offshore along this band of latitude during summer and fall (Figure 4, bottom) and very thin or no BLs along the coast in JAS.

[17] In early fall (September), the ITCZ is located around 6–8°N. As a result, it reinforces the freshening of surface

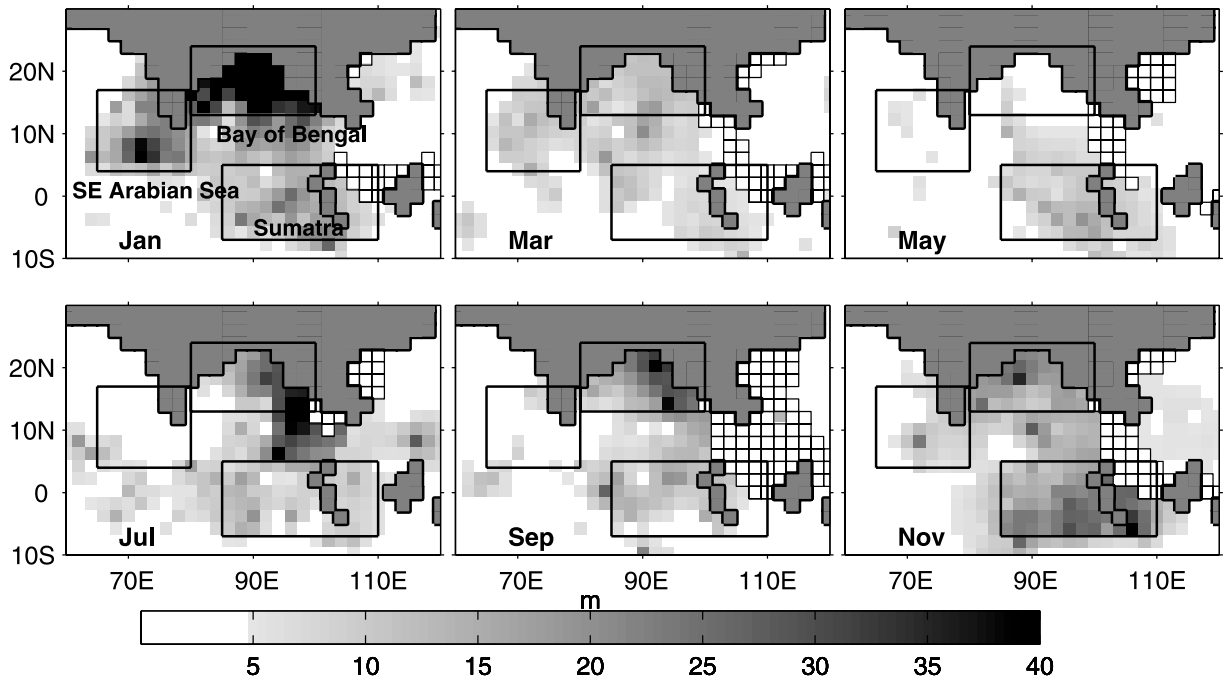

Figure 5. Monthly seasonal cycle of the barrier layer thickness (meters) in the tropical Indian Ocean. Grid points with no data are contoured in black. The boxes show the three main areas of BL occurrence in this ocean (see text for details).

waters carried by the North Equatorial Countercurrent. In early spring, it is located farther south, in the vicinity of the equator (thick black contours in Figure 4). Thus it crosses twice a year the latitude band around 3–4°N where a BL that, according to the currents direction, cannot be due to the advection of fresh waters of Amazon origin is additionally detected in boreal winter. This BL of 5 to 10 m thickness and its link to the ITCZ-induced precipitations was already described by *Foltz et al.* [2004].

[18] Large BL areas are additionally located farther poleward in winter (boxes in Figure 4). These are discussed in section 6. Finally, the thick BL located in the western tropical Atlantic is analyzed separately in section 7.

5. Northern Tropical Indian Ocean

[19] In the northern Indian Ocean (north of 10°S), the combined effect of large river runoffs, equatorial dynamics and the monsoon phenomenon results in a wide variety of processes leading to salinity anomalies and BL formations. *Sprintall and Tomczak* [1992] diagnosed three BL areas in the Indian Ocean: the Bay of Bengal, the southeastern Arabian Sea and the area off Sumatra. Below, we propose to revisit successively the seasonality of these three areas in the light of our product (Figure 5).

5.1. Bay of Bengal

[20] In agreement with observations [*Rao and Sivakumar*, 2003; *Thadathil et al.*, 2007] and model analysis [*Masson et al.*, 2002], BLs in the Bay of Bengal appear in fall in the east of the Bay with thicknesses of about 25 m, and later in winter in the west, reaching maximum thicknesses of 50 m. Using observed profiles of the upper ocean temperature and salinity, *Vinayachandran et al.* [2002] proposed that the initial freshwater input comes from river discharge and rainfall, during the summer monsoon. The freshwater plume is spread in the Bay by an eastward Ekman flow induced by the monsoon winds. Contrary to early findings [*Sprintall and Tomczak*, 1992], the BL thickness is maximum in January–February, confirming the findings of *Rao and Sivakumar* [2003] and *Thadathil et al.* [2007]. The BL that has built up from June to July becomes prominent by February in the following year (Figure 5), when the effects of hydrological forcing through intensified river discharges and local rainfall are felt the most on the near-surface layers. The different results obtained by *Sprintall and Tomczak* [1992] might be due to their time averaging. Note that the warm summer waters that have been trapped below the mixed layer and thus protected from the surface seasonal cooling are then responsible for observed subsurface maxima of more than 1.5°C [*de Boyer Montégut et al.*, 2007a, Figure 6]. This heat stored below the mixed layer contributes to counteract the following winter cooling through vertical entrainment of warm waters [*de Boyer Montégut et al.*, 2007b]. Thinner barrier layers are also present in July and August in the north of the Bay, consistent with observations of *Shetye et al.* [1996].

5.2. Southeastern Arabian Sea

[21] On the other side of the Indian Peninsula, in the southeastern Arabian Sea (65°–80°W), our climatology clearly show a barrier layer between October and March (Figure 5). As described by *Masson et al.* [2005] the low-salinity surface waters are not created locally by atmospheric fluxes, which are in the way of a net evaporation during those months over the area. Fresh surface water is advected out of

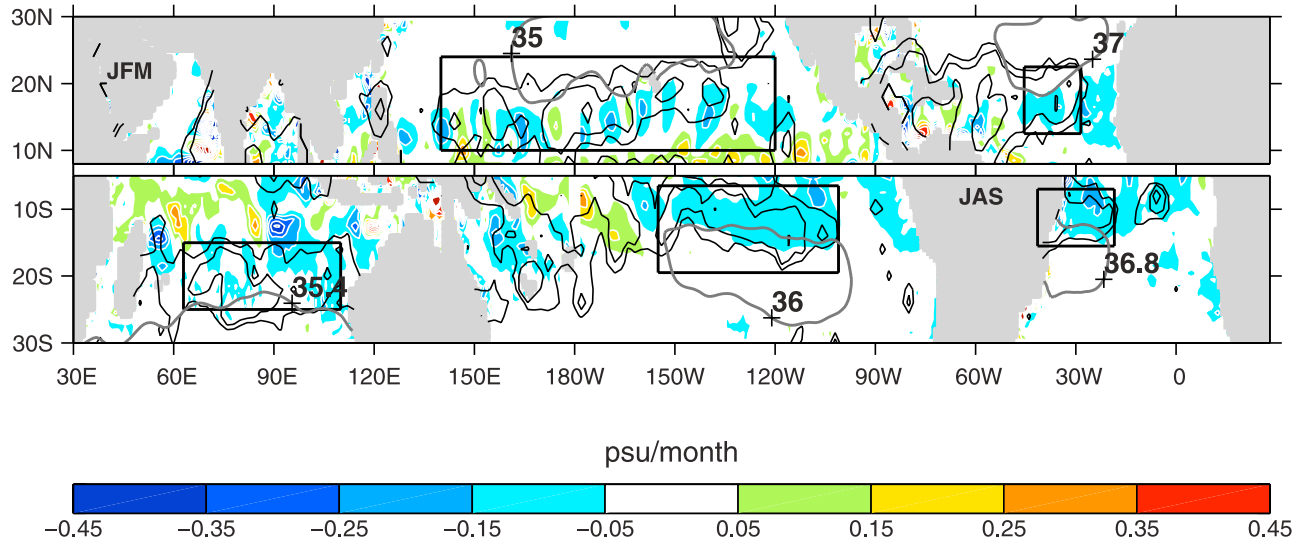

Figure 6. Colors show advection of SSS taken from WOA01 [*Conkright et al.*, 2002] by the drifter-derived near-surface currents from *Lumpkin and Garraffo* [2005] averaged over (top) January–March and (bottom) July–September. Contours are BL thickness averaged over the same seasons. Contours are drawn for thicknesses of 5 m, 10 m, and 25 m. The five boxes highlight the tropical BLs described in section 6 and used for spatial averages in Figure 7. In the Pacific and in the Atlantic, they are also shown in Figures 2 and 4, respectively. The thick gray contours show isohalines from WOA01 [*Conkright et al.*, 2002]. Only some selected isohalines for each basin are shown, in order to highlight the location of the subtropical salinity maxima.

the Bay of Bengal by the westward currents associated to the winter monsoon. This is combined with a downwelling Rossby wave and results in the formation of a thick BL [*Durand et al.*, 2007]. These BLs reach their maximum thickness of 15 to 20 m (regional average) in January–February. Subsurface waters warmer than the surface are trapped in this BL [*de Boyer Montégut et al.*, 2007a, Figure 6], consistent with work by *Thadathil and Gosh* [1992], which can impact local SSTs, the atmosphere and the onset of the monsoon season according to *Masson et al.* [2005].

5.3. Eastern Equatorial Indian Ocean

[22] Finally, BLs are present all year long in the eastern equatorial Indian Ocean and offshore Java and Sumatra. In agreement with recent findings of *Qu and Meyers* [2005], they are thickest in November. These authors however found a relatively more pronounced seasonal cycle than in our data set. This might arise from their use of a different criteria. The mechanisms yielding these BLs have been described extensively by *Masson et al.* [2002] in an ocean general circulation model and by *Qu and Meyers* [2005] using historical hydrographic and recent Argo-float profile data. BLs around 85°E/90°E are due to the advection of salinity maximum by the equatorial Wyrtki jet in autumn. Off Sumatra, they form after westward advection of fresh waters from the coastal precipitation area. These two BLs merge together to give a thick one (20 m) with maximum horizontal extent in November (Figure 5).

[23] Note that BLs are generally not found along the subtropical eastern coasts in the Atlantic and Pacific basins (Figure 1), where the mixed layer depth is very shallow because of coastal upwellings. The BL detected off Java constitutes an exception in that respect, because of the specific topography and climatology of the Indian Ocean [*Qu and Meyers*, 2005].

[24] To conclude, our product confirms the presence of BLs in the three areas of the northern tropical Indian Ocean distinguished by *Sprintall and Tomczak* [1992]. The exact seasonality as well as the occurrence of vertical temperature inversions yet rather agrees with more recent local studies. In the southern Indian Ocean, a big patch of BL near 20°S is present in austral winter, as seen in Figure 1. It is analyzed below. Its seasonality and its location is very symmetric to the ones mentioned in the Pacific around the same latitudes in both hemisphere. All these BLs are analyzed in detail in section 6.

6. BLs on the Equatorial Flank of the Subtropical Salinity Maxima

6.1. General Description

[25] We discussed in section 3.1 the presence of zonal BL areas around 10–25° latitude in both hemispheres in the Pacific. We also mentioned large BL zones in the tropical Atlantic and the south Indian Ocean, between Magadascar and Australia, during the local winter season. As illustrated on Figure 6 (contours), these BLs are located right equatorward of the subtropical salinity maxima, i.e., on their equatorial flank. In the tropical Atlantic, a thick and persistent BL area is also located farther westward, in the Atlantic warm pool. This specific zone will be discussed in the following section. We focus here on the BLs highlighted by the boxes on Figure 6. They correspond to the subtropical BLs described by *Sato et al.* [2006]. Note that the northern Indian ocean constitutes an exception in this basin symmetry because of its specific geometry (see section 5).

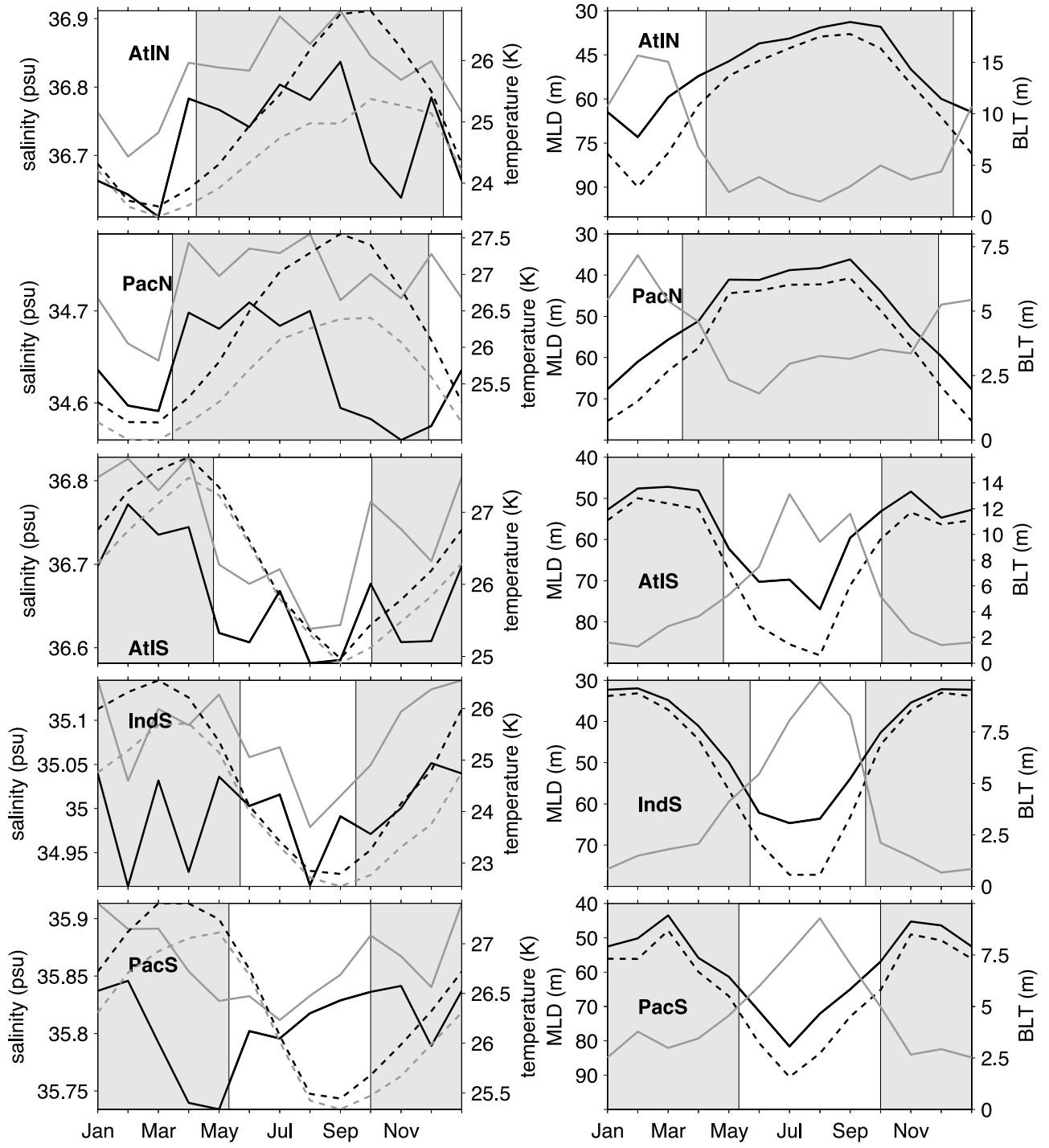

Figure 7. (left) Seasonal evolution of salinity (solid lines, left scale) and temperature (dashed lines, right scale) averaged over the boxes indicated on Figure 6. The black lines show the surface fields, and the grey lines show the corresponding field at 50 m depth. All data are taken from WOA01 [*Conkright et al.*, 2002]. The time period where no significant BL is detected (thickness less than 5 m) is shown in gray. (right) Density-based (solid line) and temperature-based (dashed line) mixed layer depth (MLD) computed with a criteria equivalent to a change of 0.2°C (left scale). Note the reversed vertical scale. The time period where no significant BL is detected (thickness less than 5 m) is shown in gray. The monthly time series of the BLT is shown in light gray (right scale).

6.2. Formation Mechanism

[26] The formation of salty Subtropical Underwater (STUW) (e.g., *Worthington* [1976] and *Blanke et al.* [2002] in the North Atlantic, *O'Connor et al.* [2002] in the North Pacific) has been proposed as the origin for the presence of BL in the northern tropical Atlantic [*Sprintall and Tomczak*, 1992]. *Sato et al.* [2004, 2006] investigated

this mechanism but could not find large-scale surface temperature and salinity horizontal gradients to relate, through subduction, to the vertical profiles. Hence they proposed that small-scale salinity fronts, found in ARGO measurements, were responsible for the strong stratification in salinity relative to the temperature. Nonetheless, we note that the same tropical BLs are finely simulated in the IPSL low-resolution (200 km) ocean general circulation model (not shown). This hypothesis is therefore likely not necessary to understand the phenomenon. We propose a modified mechanism based on the analysis of Figure 7 that shows the seasonal cycle of surface and subsurface temperature and salinity as well as the mixed layer depths and barrier layer thickness averaged over the boxes of Figure 6.

[27] During early winter, when the mixing deepens with the help of intense wind stirring and negative buoyancy forcing, the atmosphere cools the SST (Figure 7, left, dashed lines), the isothermal layer deepens (Figure 7, right, dashed lines). Meanwhile, in all the five regions, subsurface salinity is relatively high because of the presence of STUW (Figure 7, left, solid lines) while the surface salinity is maintained at a relatively low value by advection of fresh equatorial waters (Figure 6 and *Foltz et al.* [2004]) primarily by the Ekman currents [*Mignot and Frankignoul*, 2003, 2004]. These climatological fresh equatorial waters are a classic feature of all the oceans resulting from the ITCZ intense precipitations. The southern Indian Ocean is also further freshened by the Ekman advection of the upwelled low-salinity Indonesian Throughflow thermocline water [*Song et al.*, 2004]. These surface currents are nearly tangent to surface isotherms and sustain freshening only. This partly preserves a vertical salinity gradient against the winter vertical mixing in all five regions. As a result, the isothermal layer deepens faster than the density (and the salinity) mixed layer, resulting in a BL (Figure 7, right).

[28] Around February for the boreal winter and August for the austral winter, a peak of BL thickness, corresponding to a second phase of the process, is best observed for spatial averages in the Pacific and Indian oceans (Figure 7) but is also seen locally in other basins: wind stirring and negative buoyancy fluxes reduce in amplitude and the vertical extent of the mixing shoals rapidly, as evidenced by the density-based mixed layer depth decrease. Associated to the continuous surface freshening, it causes a rapid lifting of the isohaline layer, whereas the contemporary weak SST variations displayed on the left plots of Figure 7 (end of winter cooling and beginning of spring warming) does not yet generate a surface restratification: the isothermal layer stays at its maximum value for a while. This phase leads to a peak of BL thickness in late winter. In early spring, the temperature finally restratifies and temperature, salinity and density are mixed down to the same depth (Figure 7, right).

[29] Regarding the seasonality of the BL, this mechanism is consistent with work by *Sato et al.* [2006], who also hint toward a control by the buoyancy forcing, which tends to generate a maximum mixed layer in winter. The deeper the mixed layer, the deeper the isothermal layer and thus the thicker the BL when it forms. Note however that in contrast with these authors, the formation mechanism that we propose does not require the variability of subduction. It only invokes the presence of STUW which, together with the Ekman advection of fresh equatorial waters, favors a strong permanent vertical salinity gradient just below the mixed layer. Nevertheless, variability in this gradient can induce variability of the BL thickness. This could come from variability of the STUW composition or formation rate, as suggested by previous authors, or variability of the surface freshening. This latter effect is visible for example on Figure 4 of *Sato et al.* [2004]: near the end of February, the base of mixed layer shoals abruptly by 50 m as a result of both surface freshening and subsurface increase of salt. This effect contributes to modulate the BL thickness, whose existence is bounded to seasonality of the temperature stratification.

7. BLs of the North Atlantic Warm Pool

[30] In addition to the BL located in the open ocean on the equatorial flank of the salinity maximum, a large (about 1200 km $\times$ 2000 km) area of thick (exceeding 50 m) and persistent (more than 6 months) BLs is detected in the western tropical Atlantic, north of South America (90 to 60°W, 10 to 25°N, Figure 4). They are thickest in boreal winter but they persist almost all year long. This area is in fact one of the most prominent structures of the global tropics (Figure 1).

[31] In contrast to the BLs described above, this BL area is characterized, in its eastern part, by strong temperature inversions in winter (Figure 4, white contour in JFM) that can reach up to 0.6°C around 60m depth (Figure 6 of part 1 of this paper [*de Boyer Montégut et al.*, 2007a]). These inversions (centered at 60°W and 18°N) have never been explained nor described to our knowledge. They explain that separated analysis from the ones above is required, namely in comparison with BLs located on the equatorial flank of the North Atlantic salinity subtropical maximum (section 6) and the coastal BL (section 4). In particular, note that the inversion area is clearly detached from the coast. Temperature inversions are also detected at some grid points over the BLs on the equatorial flank salinity maximum (Figure 4) but they only concern isolated grid points and are much thinner (compare Figure 6 of part 1 [*de Boyer Montégut et al.*, 2007a]). In spite of this distinction, the formation mechanism of these BLs involves processes already described in the previous sections. Figure 6 illustrates that it is freshened in surface by advection. The fresh waters are transported from the Amazon and the ITCZ area probably partly by the North Brazil current, as suggested by *Ferry and Reverdin*'s [2004] in a model study, but also by northward Ekman currents and by anticyclonic eddies forming at the retroflection of the North Brazil current [*Johns et al.*, 1990]. Recent observations by *Hu et al.* [2004] indicate that the latter can indeed affect offshore areas. Further analysis (not shown) indicate that advection of fresh water into the inversion area is maximum in summer and early fall, when the mixed layer is still very warm. Summer and fall warm waters can thus be trapped beneath the fresh advected waters, inducing the detected temperature inversions. The latter are thus due to the specific seasonality of the North Brazil Current advection relative to the Ekman transport discussed in section 6.

[32] A more western maximum of BL thickness is also present in the Caribbean Sea (Figures 1 and 6). Here the

local seasonal SSS cycle is marked by a rainy period that extends from May to October, with a relative minimum in summer (e.g., *Giannini et al.* [2000] and contours in Figure 4). These strong precipitations add on the advection of fresh waters to induce BLs. Note that they are strongly modulated by the ENSO variability [e.g., *Giannini et al.*, 2000]. When the BL climatology is recomputed excluding El Niño years, these BLs are slightly thicker (not shown). In both cases, the BL weakens at the beginning of the warm season when SST and surface stratification increase again, as described in section 6.2.

8. Conclusions

[33] In the first part of this paper [*de Boyer Montégut et al.*, 2007a], we presented a new climatology of the differences in temperature and density stratification in the upper ocean to highlight the influence of salinity on this stratification. This new climatology is a global product based on the compilation of the most recent NODC, WOCE and ARGO databases. We emphasize that its main novelty as compared to previous global and large-scale studies is that it is based on profile-wise computations. This results in more realistic and detailed structures than already gridded profiles, since no merging by smoothing or interpolation is applied.

[34] In this paper, we used this climatology to analyze the latitudes equatorward of about 25° in greater detail. Several studies have already examined the occurrence of BLs at these latitudes in different oceanic basins. Since our product involves a much larger amount of profiles, direct comparison of our climatology with previous studies cannot be done systematically. A good agreement can however be viewed as a validation of the robustness of the BL patterns. Furthermore, this is the first global analysis of BL occurrence using practically all individual profiles available since 1967.

[35] In the deep tropics, i.e., equatorward of about 10° latitude, formation mechanisms are various and linked to the specific geometry of each basin. In the deep tropical Pacific we were able to distinguish a weak seasonal cycle at the equator, in relation with the eastern extension of the Warm Pool. Our analysis shows consistency with the main formation mechanisms already proposed at longer (mainly interannual) timescales: precipitations under the ITCZ and the SPCZ and subduction at the eastern edge of the Warm Pool. In the deep tropical Atlantic, intense precipitations under the ITCZ, large runoff from the Amazon river and the seasonality of the oceanic circulation also create a complex BL system, with a clear seasonal cycle. In the northern tropical Indian Ocean, numerous and thick BL zones are generated by the combined effect of large river runoffs, equatorial dynamics and the monsoon phenomenon. Seasonality (maximum in winter) and thickness (around 15 m in the Arabian Sea and offshore Sumatra, up to 45 m in the Bay of Bengal) detected in our product are very close to previous local studies. Large temperature inversions that have been presented as having an important climatic impact [*Durand et al.*, 2004; *Masson et al.*, 2005] were furthermore detected.

[36] Farther poleward but equatorward of the subtropical salinity maxima (i.e., between 10° and 25° of latitude), a strong symmetrical BL occurrence emerged. It confirms the recent findings of *Sato et al.* [2006] based on the profiles obtained by ARGO floats from January 2000 to June 2005. This symmetry extends the basin symmetry in terms of BL occurrence, seasonality, and formation mechanism found for the polar and subpolar areas by *de Boyer Montégut et al.* [2007a]. Here the intense surface freshening resulting from poleward Ekman advection of the fresh equatorial surface waters combined with the presence of subsurface salty waters lead to a strong, robust and permanent salinity stratification. In winter, the surface waters are additionally cooled by surface heat loss, so that temperature stratification is reduced. This induces BLs of up to 20 (in the South Atlantic and Indian oceans) and 30 (in the North and South Pacific and the North Atlantic) meters thick during the local winter season on the equatorial flank of the subtropical salinity maxima. In summer, the thermocline shoals under the effect of atmospheric heating and coincides again with the top of the pycnocline.

[37] Finally, the thick BLs in the western tropical North Atlantic are due to the combined effect of horizontal advection of fresh waters in fall, inducing thick temperature inversions in subsurface around 60°W–18°N, and intense precipitations in the far west (around 80°W). Note that the situation in the western part of this BL resembles that in the central subtropical basin, except that the freshwater advection isolates the subsurface waters as soon as early fall, so that they remain warmer than the winter surface, inducing the reversed temperature profiles.

[38] As stated by *de Boyer Montégut et al.* [2007a], we believe that the data set is useful for a large spectrum of oceanographic studies such as the revision of accurate upper ocean heat, salt and biological budgets. Furthermore, in several regions, mechanisms of BL formation and destruction are still not fully understood. Further analysis is for example required to better elucidate the formation mechanism of the complex BL in the western tropical Atlantic and in particular distinguish the influence of ENSO interannual variability from the seasonal cycle. Owing to the lack of data, investigation of BL mechanisms often requires the use of ocean general circulation models, that need to be validated against a reliable and robust product [e.g., *Durand et al.*, 2007]. For these reasons, we would like to make our product public. The monthly mean differences $D_{T-02} - D_\sigma$ as well as the fields D_{T-02} and D_σ can be downloaded from http://www.locean-ipsl.upmc.fr/~cdblod/blt.html.

[39] **Acknowledgments.** We would like to acknowledge the National Oceanographic Data Center, the World Ocean Circulation Experiment, and the Coriolis project for the rich publicly available databases. We are grateful to Gilles Reverdin for stimulating discussions, constructive comments, and encouragements and to Fabien Durand and Roger Lukas for detailed comments on the manuscript. We also thank Kanako Sato for constructive comments. CBM was partly supported by a DGA grant (DGA-CNRS 2001292) and by funding of the Programme National d'Étude de la Dynamique et du Climat (PNEDC).

References

Ando, K., and M. J. McPhaden (1997), Variability of surface layer hydrography in the tropical Pacific Ocean, *J. Geophys. Res.*, *102*(C10), 23,063–23,078.

Blanke, B., M. Arhan, A. Lazar, and G. Prévost (2002), A Langrangian numerical investigation of the origins and fates of the salinity maximum

water in the Atlantic, *J. Geophys. Res.*, *107*(C10), 3163, doi:10.1029/2002JC001318.

Bonjean, F., and G. S. E. Lagerloef (2002), Diagnostic model and analysis of the surface currents in the tropical Pacific Ocean, *J. Phys. Oceanogr.*, *32*(10), 2938–2954.

Condie, S. A. (1991), Separation and recirculation of the North Brazil Current, *J. Mar. Res.*, *49*, 1–19.

Conkright, M. E., R. A. Locarnini, H. E. Garcia, T. D. O'Brien, T. P. Boyer, C. Stephens, and J. I. Antonov (2002), *World Ocean Atlas 2001: Objective Analyses, Data Statistics, and Figures*, *CD-ROM Documentation*, vol. 17, NOAA Silver Spring, Md.

Cronin, M. F., and M. J. McPhaden (2002), Barrier layer formation during westerly wind bursts, *J. Geophys. Res.*, *107*(C12), 8020, doi:10.1029/2001JC001171.

de Boyer Montégut, C., G. Madec, A. S. Fisher, A. Lazar, and D. Iudicone (2004), Mixed layer depth over the global ocean: An examination of profile data and a profile-based climatology, *J. Geophys. Res.*, *109*, C12003, doi:10.1029/2004JC002378.

de Boyer Montégut, C., J. Mignot, A. Lazar, and S. Cravatte (2007a), Control of salinity on the mixed layer depth in the world ocean: Part 1: General description, *J. Geophys. Res.*, *107*, C06011, doi:10.1029/2006JC003953.

de Boyer Montégut, C., J. Vialard, S. S. C. Shenoi, D. Shankar, F. Durand, C. Ethé, and G. Madec (2007b), Simulated seasonal and interannual variability of mixed layer heat budget in the northern Indian Ocean, *J. Clim.*, *20*, 3249–3268.

Delcroix, T., and M. McPhaden (2002), Interannual sea surface salinity and temperature changes in the western Pacific warm pool during 1992–2000, *J. Geophys. Res.*, *107*(C12), 8002, doi:10.1029/2001JC000862.

Delcroix, T., L. Gourdeau, and C. Hénin (1998), Sea surface salinity changes along the Fiji-Japan shipping track during the 1996 La Niña and 1997 El Niño period, *Geophys. Res. Lett.*, *25*(16), 3169–3172.

Durand, F., L. Gourdeau, T. Delcroix, and J. Verron (2002), Assimilation of sea surface salinity in a tropical Oceanic General Circulation Model (OGCM): A twin experiment, *J. Geophys. Res.*, *107*(C12), 8004, doi:10.1029/2001JC000849.

Durand, F., S. R. Shetye, J. Vialard, D. Shankar, S. S. C. Shenoi, C. Ethe, and G. Madec (2004), Impact of temperature inversion on SST evolution in the South-Eastern Arabian Sea during the pre-summer monsoon season, *Geophys. Res. Lett.*, *31*, L01305, doi:10.1029/2003GL018906.

Durand, F., D. Shankar, C. de Boyer Montégut, S. S. C. Shenoi, B. Blanke, and G. Madec (2007), Modeling the barrier-layer formation in the South-Eastern Arabian Sea, *J. Clim.*, *20*, 2109–2120.

Ferry, N., and G. Reverdin (2004), Sea surface salinity interannual variability in the western tropical Atlantic: An ocean general circulation model study, *J. Geophys. Res.*, *109*, C05026, doi:10.1029/2003JC002122.

Foltz, G. R., S. A. Grodsky, J. A. Carton, and M. J. McPhaden (2004), Seasonal salt budget of the northwestern tropical Atlantic Ocean along 38°W, *J. Geophys. Res.*, *109*, C03052, doi:10.1029/2003JC002111.

Giannini, A., Y. Kushnir, and M. C. Cane (2000), Interannual variability of Caribbean rainfall, ENSO, and the Atlantic Ocean, *J. Clim.*, *13*, 297–310.

Harrison, D. E., and G. A. Vecchi (1997), Westerly wind events in the tropical Pacific, 1986–1995, *J. Clim.*, *10*, 3131–3156.

Hénin, C., Y. du Penhoat, and M. Ioualalen (1998), Observations of sea surface salinity in the western Pacific fresh pool: Large scale changes during 1992–1995, *J. Geophys. Res.*, *103*(C4), 7523–7536.

Hu, C., E. T. Montgomery, R. W. Schmitt, and F. E. Muller-Karger (2004), The dispersal of the Amazon and Orinocco River water in the tropical Atlantic and Caribbean Sea: Observation from space and S-PALACE floats, *Deep Sea Res., Part II*, *51*, 1151–1171.

Johns, W. E., T. N. Lee, F. Schott, R. J. Zantopp, and R. H. Evans (1990), The north Brazil current retroflection: Seasonal structure and eddy variability, *J. Geophys. Res.*, *95*(C12), 22,103–22,120.

Lentz, S. J. (1995), Seasonal variations in the horizontal structure of the Amazon plume inferred from historical hydrographic data, *J. Geophys. Res.*, *100*(C2), 2391–2400.

Lewis, M. R., M. E. Carr, G. C. Feldman, W. Esaias, and C. McClain (1990), Influence of penetrating solar radiation on the heat budget in the equatorial Pacific Ocean, *Nature*, *347*, 543–545.

Lukas, R., and E. Lindstrom (1991), The mixed layer of the western equatorial Pacific Ocean, *J. Geophys. Res.*, *96*(Supplement), 3343–3357.

Lumpkin, R., and Z. Garraffo (2005), Evaluating the decomposition of tropical Atlantic drifter 10 observations, *J. Atmos. Oceanic Technol.*, *22*, 1403–1415.

Maes, C., J. Picaut, and S. Belamari (2002), Salinity barrier layer and onset of El Niño in a Pacific coupled model, *Geophys. Res. Lett.*, *29*(24), 2206, doi:10.1029/2002GL016029.

Maes, C., J. Picaut, A. Kentaro, and K. Yoshifumi (2004), Characteristics of the convergence zone at the eastern edge of the Pacific warm pool, *Geophys. Res. Lett.*, *31*, L11304, doi:10.1029/2004GL019867.

Maes, C., J. Picaut, and S. Belamari (2005), Importance of salinity barrier layer for the build up of El Niño, *J. Clim.*, *18*, 104–118.

Maes, C., K. Ando, T. Delcroix, W. S. Kessler, M. J. McPhaden, and D. Roemmich (2006), Observed correlation of surface salinity, temperature and barrier layer at the eastern edge of the western Pacific warm pool, *Geophys. Res. Lett.*, *33*, L06601, doi:10.1029/2005GL024772.

Masson, S., and P. Delecluse (2001), Influence of the Amazon river runoff on the tropical Atlantic, *Phys. Chem. Earth, Part B*, *26*(2), 137–142.

Masson, S., P. Delecluse, J.-P. Boulanger, and C. Menkes (2002), A model study of the seasonal variability and formation mechanisms of the barrier layer in the equatorial Indian Ocean, *J. Geophys. Res.*, *107*(C12), 8017, doi:10.1029/2001JC000832.

Masson, S., et al. (2005), Impact of barrier layer on winterspring variability of the southeastern Arabian Sea, *Geophys. Res. Lett.*, *32*, L07703, doi:10.1029/2004GL021980.

Meinen, C., and M. J. McPhaden (2000), Observations of warm water volume changes in the equatorial Pacific and their relationship to El Niño and La Niña, *J. Clim.*, *13*, 3551–3559.

Mignot, J., and C. Frankignoul (2003), On the interannual variability of surface salinity in the Atlantic, *Clim. Dyn.*, *20*, 555–565.

Mignot, J., and C. Frankignoul (2004), Interannual to interdecadal variability of sea surface salinity in the Atlantic and its link to the atmosphere in a coupled model, *J. Geophys. Res.*, *109*, C04005, doi:10.1029/2003JC002005.

O'Connor, B. M., R. A. Fine, K. A. Maillet, and D. B. Olson (2002), Formation rates of subtropical underwater in the Pacific Ocean, *Deep Sea Res., Part I*, *49*, 1571–1590.

Pailler, K., B. Bourles, and Y. Gouriou (1999), The barrier layer in the western tropical Atlantic Ocean, *Geophys. Res. Lett.*, *26*(14), 2069–2072.

Picaut, J., M. Ioualalen, T. Delcroix, F. Masia, R. Murtugudde, and J. Vialard (2001), The oceanic zone of convergence on the eastern edge of the Pacific warm pool: A synthesis of results and implications for El Niño–Southern Oscillation and biological phenomena, *J. Geophys. Res.*, *106*(C2), 2363–2386.

Qu, T., and G. Meyers (2005), Seasonal variation of barrier layer in the southeastern tropical Indian Ocean, *J. Geophys. Res.*, *110*, C11003, doi:10.1029/2004JC002816.

Rao, R. R., and R. Sivakumar (2003), Seasonal variability of sea surface salinity and salt budget of the mixed layer of the north Indian Ocean, *J. Geophys. Res.*, *108*(C1), 3009, doi:10.1029/2001JC000907.

Reverdin, G., C. Frankignoul, E. Kestenare, and M. J. McPhaden (1994), Seasonal variability in the surface currents of the equatorial Pacific, *J. Geophys. Res.*, *99*(C10), 20,323–20,344.

Sato, K., T. Suga, and K. Hanawa (2004), Barrier layer in the North Pacific subtropical gyre, *Geophys. Res. Lett.*, *31*, L05301, doi:10.1029/2003GL018590.

Sato, K., T. Suga, and K. Hanawa (2006), Barrier layer in the subtropical gyres of the world's oceans, *Geophys. Res. Lett.*, *33*, L08603, doi:10.1029/2005GL025631.

Shetye, S. R., A. D. Gouveia, D. Shankar, S. S. C. Shenoi, P. N. Vinayachandran, D. Sundar, G. S. Michael, and G. Nampoothiri (1996), Hydrography and circulation in the western Bay of Bengual during the northeast monsoon, *J. Geophys. Res.*, *101*(C6), 14,011–14,025.

Shinoda, T., and R. Lukas (1995), Lagrangian mixed laxer modelling of the western equatorial Pacific, *J. Geophys. Res.*, *100*(C2), 2523–2541.

Song, Q., A. L. Gordon, and M. Visbeck (2004), Spreading of the Indonesian throughflow in the Indian Ocean, *J. Phys. Oceanogr.*, *34*(4), 772–792.

Sprintall, J., and M. Tomczak (1992), Evidence of the barrier layer in the surface layer of the tropics, *J. Geophys. Res.*, *97*(C5), 7305–7316.

Thadathil, P., and A. K. Gosh (1992), Surface layer temperature inversion in the Arabian Sea during winter, *J. Oceanogr.*, *48*, 293–304.

Thadathil, P., P. M. Muraleedharan, R. R. Rao, Y. K. Somayajulu, G. V. Reddy, and C. Revichandran (2007), Observed seasonal variability of barrier layer in the Bay of Bengal, *J. Geophys. Res.*, *112*, C02009, doi:10.1029/2006JC003651.

Vialard, J., and P. Delecluse (1998a), An OGCM study for the TOGA decade. Part 1: Role of salinity in the physics of the western Pacific fresh pool, *J. Phys. Oceanogr.*, *28*(6), 1071–1088.

Vialard, J., and P. Delecluse (1998b), An OGCM study for the TOGA decade. Part 2: Barrier-layer 31 formation and variability, *J. Phys. Oceanogr.*, *28*(6), 1089–1106.

Vinayachandran, P. N., V. S. N. Murty, and V. Ramesh Babu (2002), Observations of barrier layer formation in the Bay of Bengal during summer monsoon, *J. Geophys. Res.*, *107*(C12), 8018, doi:10.1029/2001JC000831.

Woods, J. D., W. Barkmann, and A. Horch (1984), Solar heating of the oceans—Diurnal, seasonal and meridional variations, *Q. J. R. Meteorol. Soc.*, *110*, 633–656.

Worthington, L. V. (1976), *On the North Atlantic Circulation*, *Johns Hopkins Oceanogr. Stud.*, vol. 6, 110 pp., Johns Hopkins Univ. Press, Baltimore, Md.

Wyrtki, K. (1975), El Niño—The dynamic response of the equatorial Pacific to the atmospheric forcing, *J. Phys. Oceanogr.*, *5*(4), 572–584.

Xie, P., and P. A. Arkin (1997), A 17-year monthly analysis based on gauge observations, satellite estimates and numerical model outputs, *Bull. Am. Meteorol. Soc.*, *78*(11), 2539–2558.

You, Y. (1995), Salinity variability and its role in the barrier-layer formation during TOGACOARE, *J. Phys. Oceanogr.*, *25*(11), 2778–2807.

Yu, X., and M. J. McPhaden (1999), Seasonal variability in the equatorial Pacific, *J. Phys. Oceanogr.*, *29*(5), 925–947.

S. Cravatte, Laboratoire d'Etudes en Géophysique et Océanographie Spatiales, Unité Mixte de Recherche, CNRS/IRD/CNES/Université Paul Sabatier, 14, av. Edouard Belin, F-31400 Toulouse, France.

C. de Boyer Montégut, Frontier Research Center for Global Change, Japan Agency for Marine-Earth Science and Technology, 3173-25 Showa-machi, Kanazawa-ku, Yokohama, Kanagawa 236-0001, Japan.

A. Lazar and J. Mignot, Laboratoire d'Océanographie et du Climat: Expérimentations et Approches Numériques, Unité Mixte de Recherche, CNRS/IRD/UPMC/MNHN, Institut Pierre Simon Laplace, Case 100, 4 place Jussieu, F-75252 Paris Cedex 05, France. (juliette.mignot@locean-ipsl.upmc.fr)